Nontrivial resource requirement in the early stage for containment of epidemics

Xiaolong Chen,[1,2,3,*] Tianshou Zhou,[4,*] Ling Feng,[5,6,*] Junhao Liang,[4] Fredrik Liljeros,[7] Shlomo Havlin,[8] and Yanqing Hu[1,3,†]

[1]*School of Data and Computer Science, Sun Yat-sen University, Guangzhou 510006, China*

[2]*Web Sciences Center, University of Electronic Science and Technology of China, Chengdu 611731, China*

[3]*Big Data Research Center, University of Electronic Science and Technology of China, Chengdu 611731, China*

[4]*School of Mathematics, Sun Yat-sen University, Guangzhou 510006, China*

[5]*Institute of High Performance Computing, A*STAR, 138632 Singapore*

[6]*Department of Physics, National University of Singapore, 117551 Singapore*

[7]*Department of Sociology, Stockholm University, 17177 Stockholm, Sweden*

[8]*Department of Physics, Bar-Ilan University, Ramat-Gan 52900, Israel*

(Received 13 October 2018; revised manuscript received 10 July 2019; published 23 September 2019)

During epidemic control, containment of the disease is usually achieved through increasing a devoted resource to reduce the infectiousness. However, the impact of this resource expenditure has not been studied quantitatively. For disease spread, the recovery rate can be positively correlated with the average amount of resource devoted to infected individuals. By incorporating this relation we build a novel model and find that insufficient resource leads to an abrupt increase in the infected population size, which is in marked contrast with the continuous phase transitions believed previously. Counterintuitively, this abrupt phase transition is more pronounced in less contagious diseases. Furthermore, we find that even for a single infection source, the public resource needs to be available in a significant amount, which is proportional to the total population size, to ensure epidemic containment. Our findings provide a theoretical foundation for efficient epidemic containment strategies in the early stage.

DOI: 10.1103/PhysRevE.100.032310

I. INTRODUCTION

Epidemic outbreaks have detrimental impacts globally on both public health and social activities [1–4]. Understanding of the mechanism of epidemic spreading involved with human activities is a crucial issue [5–9]. Previous studies on epidemic spreading have mostly focused on the impact of contact network structure [10–14], individual mobility [7,8], and various other aspects of the spreading process [15–22]. Usually, the spreading power has been considered to be constant throughout the entire spreading process. However, the spreading power is not constant, as commonly assumed, but highly influenced by the resources invested to contain the spreading. The effect of resource-dependent spreading power has been largely overlooked in the past, in contrary to the real dynamics. Recently, the impact of the infected population on the remaining available human resources and its influence on epidemics have been studied [23], and it has been found that explosive epidemic outbreaks are due to the reduced productivity output from the total population, when a significant portion of the population is infected. However, in modern societies, it is extremely rare for diseases to be so widespread, due to heightened government surveillance [24,25] and prompt containment actions [7,26] of their spreading at the early stage. Yet diseases can still be fatal and affect the lives of thousands or even millions of people. Thus, the amount of public resource expenditure during the early stage is of critical concern.

The devoted resources can have different influences on epidemic spreading. But many of these different influences will effectively reduce the infectiousness of a disease in a population. For example, they can shorten the duration of the infected or identify a higher fraction of the infected population that requires intervention and, consequently, decrease the spreading power. The duration of infectiousness is not necessarily the same as the duration of being sick. Infected individuals may become infectious before showing any symptoms such as those with the yearly flu. Some infections may not show any symptoms, such as *Chlamydia trichomatis* [27]. The possibility of shortening the duration of contagiousness varies for different diseases and can be medical, such as quick identification, quarantine, and cure of the infected population, as well as social, such as good insurance for loss of income, which may motivate the staff at a workplace to stay at home when sick and hence shorten the duration of infectiousness at the workplace. Identifying a higher fraction of the infected can be achieved through subsidization of screening costs. Common to most methods is that their implementation has a cost. Hence, it greatly depends on the devoted resource. This is critical, in particular, in the case of fatal diseases, which usually attract more public attention and more resources in their containment. In this work we simplify the effects of an increased resource amount into a reduced infectious rate and study its impact on the dynamics of the generic susceptible-infected-susceptible (SIS) model, as well as the spreading outcome.

*These authors contributed equally to this work.

†huyanq@mail.sysu.edu.cn

II. MODEL AND ANALYSIS

A. Resource-dependent recovery rate

Regarding the relationship between the devoted resource R and the recovery rate μ, on one hand, if the amount of the resource is limited, i.e., R is a fixed value, the overall recovery rate of the system is closely related to the infected population size ρ. Namely, the larger the infected population, the less resource per infected individual to share and, hence, the smaller the chance that the infected individual will recover. On the other hand, if the quantity of the infected population is constant at the moment, the recovery rate will be improved by properly increasing the investment of resource. This implies that the recovery rate function $\mu(R, \rho)$ is a monotonic increasing function of R and a decreasing function of ρ, such that the more total resource (or fewer infected people sharing the resource), the faster the recovery rate. Moreover, the value of μ should be constrained between 0 and 1 when R and ρ are positive. These two basic properties reflect the relations between R, ρ, and recovery rate. One example is cholera. From the recorded data in 1996 over 72 countries, the recovery rate μ of cholera—defined as $1-\mathrm{CFR}$ (case fatality rate)—is negatively related to the infected population size by average wealth per capita (PPP; purchasing power parity). Such a relationship between the recovery rate μ and the devoted resource R can be approximately fitted into the functional form of $\mu(t)$ (see Fig. 1),

$$\mu(t) = e^{-\rho(t)c/R}, \tag{1}$$

where c is the coefficient representing the relative importance of R and ρ. black Note that cholera spreads through contaminated water and food, such that it is not a direct human-to-human spreading process. Yet the recovery rate data support our intuitive assumption that the recovery rate is positively influenced by social resources.

Alternatively, we can also consider the recovery rate from the perspective of successfully identifying and quarantining the infected population. As we know, one of the most efficient ways to contain disease spreading is to isolate the infected population in the early stage of the disease outbreak. To achieve this purpose, large amounts of social and medical resources are needed to screen the population at scale. We assume that if ΔR resource is devoted to the population for screening and quarantining, the chance that an infected individual will be identified and successfully quarantined is $\frac{c\Delta R}{\rho(t)}$. Thus with the total resource R devoted, if we consider the recovery rate $\mu(t)$ as successful identification and quarantine of the infected, it can be written as

$$\mu(t) = 1 - \left(1 - \frac{c\Delta R}{\rho(t)}\right)^{\frac{R}{\Delta R}}. \tag{2}$$

In the limit ΔR is indefinitely small, i.e., $\Delta R \to 0$, we have

$$\mu(t) = \lim_{\Delta R \to 0} 1 - \left(1 - \frac{c\Delta R}{\rho(t)}\right)^{\frac{R}{\Delta R}} = 1 - e^{\frac{-cR}{\rho(t)}}. \tag{3}$$

Note that both forms of recovery rate [Eqs. (1) and (3)] are proportional to the amount of devoted resource and inversely proportional to the size of the infected population and are constrained in the range (0,1). And the usage of either one does not cause a qualitative difference as shown in Fig. 2. Here we want to qualitatively show the positive relation between the resources per infected shared (R/ρ) and the curative rate rather than the exact quantitative relation. Thus, without loss of generality, in this paper we only discuss Eq. (1), for its simplicity as well as some empirical evidence. Additionally, to illustrate qualitatively the effect of resource R on disease spreading, we use the generic spreading model with SIS

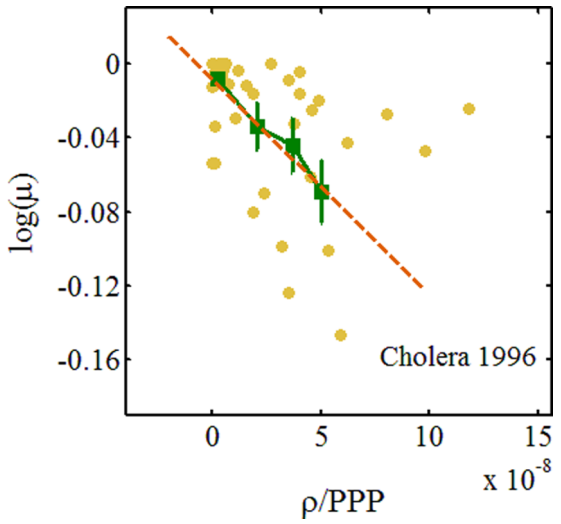

FIG. 1. Relationship between the logarithm of the cholera recovery rate μ and the size of the infected population ρ divided by the PPP in 1996, during which cholera was widespread, with 144 727 infected cases and 6418 deaths. Each yellow circle corresponds to a particular country. Green squares represent the average values of each bin of different ρ/PPP values after using the bootstrap method [28] to sample, which is suitable for the small sample size here. Then we use linear regression to fit these average values. The slope of the fitted straight line is -0.012 in the axis unit of 10^{-8} and the fitting is statistically significant, with a correlation coefficient $R^2 = 0.9723$ and a p value of 2.785×10^{-5} (fitting the average value; filled squares). There is a clear negative correlation between the logarithmic value of the recovery rate and the density of the infected population. The straight orange line is thus Eq. (1) with parameter $c = -0.012$.

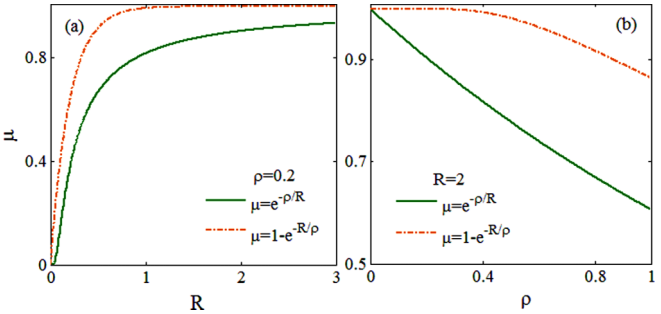

FIG. 2. Comparison of the properties of the recovery functions given by Eqs. (1) and (3). (a) Recovery rate μ as a function of resource R with a fixed infected population $\rho = 0.2$. (b) Recovery rate μ as a function of the infected population ρ with fixed resource $R = 2$. The two equations give qualitatively similar monotonic trends and both have μ values bounded in (0,1).

dynamics [10–13], which is among those commonly used in the literature for disease spreading. To simulate the effect of a fixed amount of resources, the recovery rate varies with time depending on the average amount of resource that each infected individual gets.

B. Theoretical analysis

Considering a system of N individuals embedded in a contact network, an infected individual (or node) has a probability β of spreading the disease to a neighbor with whom he or she shares a link. At the same time, the infected node has a probability of $\mu(t) = e^{-\rho(t)/R}$ [corresponding to Eq. (1) with $c = 1$] of recovering to a susceptible state, such that it does not carry the disease until it is reinfected again. Therefore the probability $p_i(t)$ that a node i is infected at time t can be described by the dynamical equation

$$\frac{dp_i(t)}{dt} = (1 - q_i(t))(1 - p_i(t)) - e^{-\rho(t)/R} p_i(t), \qquad (4)$$

where $q_i(t) = \prod_{j=1}^{N}(1 - a_{ij}\beta p_j(t))$ is the probability that node i is not infected by any of its neighbors at time t. The parameter a_{ij} denotes the adjacency matrix of the contact network and has a binary value. It is 1 when node j shares a link with node i and 0 otherwise. The infected population fraction of the whole population is $\rho(t) = \frac{1}{N}\sum_{i=1}^{N} p_i(t)$ at time t. One of the main quantities we wish to address using this equation is to study the infected population size at steady state, i.e., $\rho(\infty)$, and how it changes with the total amount of resource R.

To further analyze Eq. (4), we assume that the underlying network has degree distribution $P(k)$. With the mean-field approximation, the dynamical equation, Eq. (4), can be reduced to

$$\begin{aligned}\frac{d\rho(k,t)}{dt} &= (1 - (1 - \beta\Theta)^k)(1 - \rho(k,t)) - e^{-\rho(t)/R}\rho(k,t) \\ &\approx k\beta\Theta(1 - \rho(k,t)) - e^{-\rho(t)/R}\rho(k,t). \qquad (5)\end{aligned}$$

The approximation on the right holds when $\beta\Theta$ is close to 0. Here, $\rho(k,t)$ is the infected fraction within the nodes with degree k at time t. The first term $[1 - (1 - \beta\Theta)^k)(1 - \rho(k,t)]$ is the probability that a susceptible node with degree k gets infected through at least one of its k neighbors. The second term $e^{-\rho(t)/R}\rho(k,t)$ is the probability that an infected node will recover. Θ denotes the probability that a randomly chosen edge leads to an infected node. When the degree correlation of the network is not taken into consideration, Θ takes the form

$$\Theta = \sum_k \frac{kP(k)\rho(k,t)}{\langle k\rangle}. \qquad (6)$$

Now the total infected fraction $\rho(t)$ can be given by $\rho(t) = \sum_k P(k)\rho(k,t)$. In general, $\rho(\infty)$ cannot be analytically deduced from Eq. (5). However, in the following two typical cases, $\rho(\infty)$ can be given analytically. The first case is the homogeneous degree distribution with $P(k) = \delta_{k,\langle k\rangle}$, for which every node has the same degree. The second case is the heterogeneous power-law degree distribution $P(k) = \frac{2m^2}{k^3}$ (we mainly consider the case of exponent 3, for simplicity), where m is the minimum degree of the nodes.

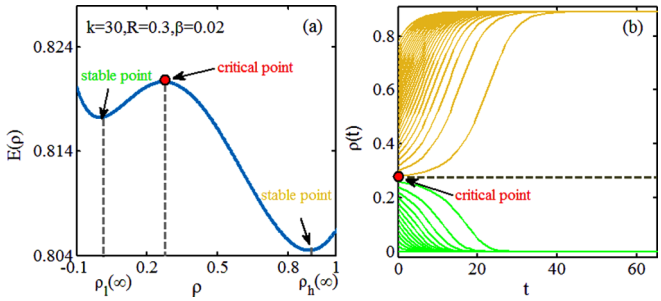

FIG. 3. Two-phase behavior with respect to the initial infection fraction $\rho(0)$. (a) Stability discussion from the potential energy perspective. Local minima correspond to stable steady states and local maxima are unstable steady states. (b) Time evolution of $\rho(t)$ with different initial values of $\rho(0)$. Depending on the initial infection fraction, the final infection fraction will converge to one of the two stable points.

For the homogeneous case, the dynamical equation, Eq. (5), can be reduced to

$$\frac{d\rho(t)}{dt} = (1 - (1 - \beta\rho(t))^k)(1 - \rho(t)) - e^{-\rho(t)/R}\rho(t). \qquad (7)$$

Note that $(1 - \beta\rho)^k \approx 1 - k\beta\rho$ for $\beta\rho \ll 1$, Eq. (7), can be further reduced to

$$\frac{d\rho(t)}{dt} = k\beta\rho(t)(1 - \rho(t)) - e^{-\rho(t)/R}\rho(t). \qquad (8)$$

The final infected population is the solution of Eq. (8) at steady state determined by $\frac{d\rho(t)}{dt} = 0$. Yet unlike the typical SIS dynamics, Eq. (8) can have multiple steady states. One can visualize the system by introducing a potential function [29] constructed from Eq. (8) as

$$E(\rho) = -\int \frac{d\rho(t)}{dt} d\rho. \qquad (9)$$

This system has one unstable (local maximum or critical) point ρ_c and two stable fixed (local minimum) points, $\rho_l(\infty)$ and $\rho_h(\infty)$, which are separated by the unstable point ρ_c as indicated in Fig. 3. As shown in Fig. 3(a), if $\rho(0)$ is to the left of the critical point ρ_c, the infected population size evolves to the left stable point at $\rho_l(\infty) = 0$; otherwise the system will evolve to the right stable point of $\rho_h(\infty) = 0.89$. Therefore when R is fixed, the two-phase behavior of the final infection population $\rho(\infty)$ dependent on the initial infected population $\rho(0)$ is separated by the critical ρ_c as shown in Fig. 3(b). That is, for a given resource value R, when $\rho(0) < \rho_c$ the epidemic can be well controlled; otherwise the epidemic will outbreak and influence a significant fraction of the population. On the other hand, this also indicates the existence of a critical value R_c for the resource parameter R for each initial condition $\rho(0)$. R_c can be obtained by finding the local maximum point though the following two equations:

$$\begin{aligned}\dot{\rho}(t) = \left.\frac{d\rho(t)}{dt}\right|_{\rho(0)} &= 0, \\ \left.\frac{\partial\dot{\rho}(t)}{\partial\rho}\right|_{\rho(0)} &> 0.\end{aligned} \qquad (10)$$

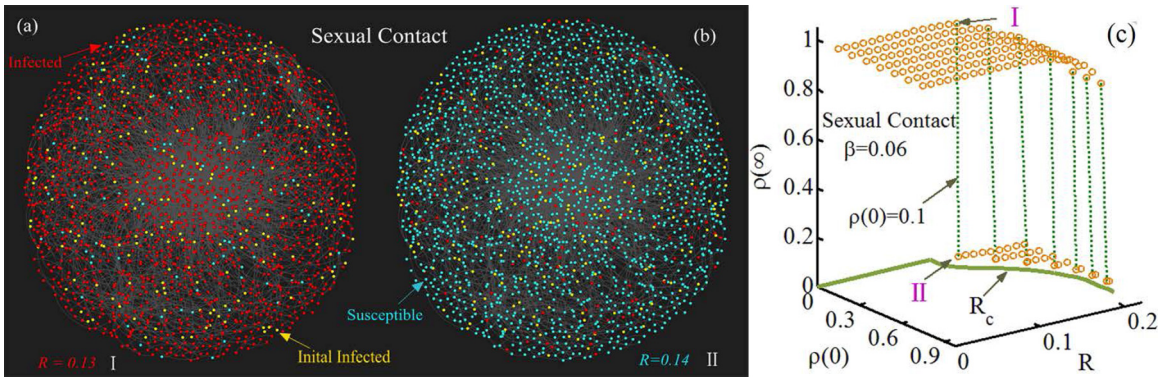

FIG. 4. Catastrophic epidemic spread due to inadequate resource R simulated on the real sexual contact network. (a, b) The simulation is carried out with $\rho(0) = 0.1$ and $\beta = 0.06$. Yellow, red, and blue nodes are the initially infected, finally infected, and susceptible nodes, respectively. Near the critical point $R_c \approx 0.135$, with a small change in R, from 0.13 to 0.14, the infected population decreases drastically. (c) The critical amount of resource R_c that separates the two phases is dependent on the initial fraction of the infected population $\rho(0)$. There is a critical R_c such that when $R < R_c$ the disease would spread to a significant fraction of the population as shown in region I, whereas when $R > R_c$ the disease would be well contained within a negligible fraction of the population as shown in controllable region II. As $\rho(0)$ increases, the minimum amount of resource R_c also increases to ensure that the disease is not widespread.

When the resource is below R_c, the disease will be widespread; otherwise it will be effectively contained.

For the heterogeneous case, at the steady state of Eq. (5), we have $\rho(k,t) = \frac{\beta k\Theta}{e^{-\rho(t)/R}+\beta k\Theta}$. Using the expression of Θ in Eq. (6) and $P(k) = \frac{2m^2}{k^3}$, considering the large node size limit, and using the integral to approximate the summation over k, we obtain the self-consistent equation for computing Θ:

$$\Theta = \int_m^\infty \frac{m\Theta\beta}{k(e^{-\rho(t)/R} + \beta k\Theta)} dk. \tag{11}$$

The integral can be computed directly to yield $\Theta = \frac{\varphi}{e^{\varphi}-1}$, where $\varphi = \frac{2e^{-\rho(t)/R}}{\beta\langle k\rangle}$. The total fraction of infected nodes can be obtained by $\rho(t) = \sum_{k=m}^{\infty} P(k)\rho(k,t)$. Substituting Eq. (5) into it, we have the equation for the fraction of infected nodes as

$$\frac{d\rho(t)}{dt} = \langle k\rangle\beta\Theta(1-\Theta) - e^{-\rho(t)/R}\rho(t), \tag{12}$$

which gives $\rho(t) = \frac{\langle k\rangle\beta\Theta(1-\Theta)}{e^{-\rho/R}}$ at steady state. Thus, we get the final result that ρ is determined by the self-consistent equation $\rho = \Phi(\rho)$ with $\Phi(\rho) = \frac{2(e^{\varphi}-\varphi-1)}{(e^{\varphi}-1)^2}$. Moreover, it can be shown that $\Phi'(\rho_0) < 1$ implies that the infected state ρ_0 is stable, while $\Phi'(\rho_0) > 1$ implies that it is unstable. Since the above analysis is not limited to the specific functional form of the recovery rate $\mu(t)$, it is easy to generalize the above analysis to the case of a general recovery rate (see the Appendix, Sec. B, for details).

III. RESULTS

A. Critical resource amount

To illustrate the impact of resources, we use the real sexual contact network [5,20] as the underlying network and simulate the resource-dependent spreading dynamics according to Eq. (4). We also use other empirical and theoretical networks comprising both heterogeneous and homogeneous degree distributions for more comprehensive investigations. Surprisingly, the model shows a bimodal outcome depending on the resource R available. As shown in Fig. 4, either the final infected population is extremely widespread to a considerable fraction of the network or only a few nodes are being infected. At a critical point of resource amount R_c, a tiny change in the resource variable R would make a huge difference in $\rho(\infty)$. Such an abrupt transition indicates that adequate critical resource is needed to fight the disease spread, since it can bring a potentially catastrophic epidemic down to a tiny outbreak (see Fig. 4). This is a signature of the first-order phase transition related to the resource available. It implies that the public resource expenditure has a critical behavior: When it is above this critical value, the disease can be effectively eradicated or contained; otherwise it cannot contain the outbreak but only slightly reduce the infected population size. *This abrupt transition is our first main finding*. In addition to this example of an abrupt transition found in the real sexual contact network, we find the same abrupt transition due to resource R in several other typical social networks, including the New Orleans Facebook network, Twitter network, and Weibo network, which could approximate real contact networks, as well as artificial networks like the Erdös-Rényi and scale-free networks (see Fig. 5).

We show the abrupt jump size $J(R_c)$ vs β for the real sexual contact network in Fig. 6(a) and that for the other networks in Fig. 5(c). One can see that when β is large enough, the jump size $J(R_c)$ at the critical resource value R_c diminishes to 0. This means that for large β values, the infected population size drops continuously with increases in the devoted resource but discontinuously when β is small. This phenomenon can also be found in other empirical networks (see the Appendix, Sec. A, for details) and random networks (see Fig. 7). The boundary value β_b is the lowest β value for which the infected population changes continuously vs the resource amount at R_c [i.e., the points where $J(R_c) = 0$ in Fig. 6(a) and for other

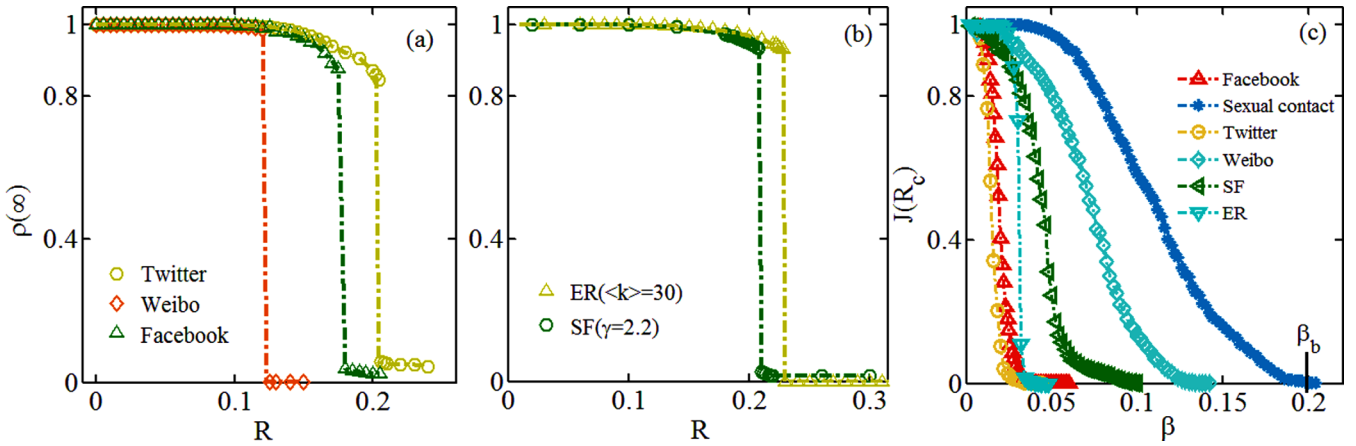

FIG. 5. Catastrophic outbreaks in different networks due to resource inadequacy. With an increasing amount of resource R devoted to constraint of the spreading, the final infected population size $\rho(\infty)$ suddenly drops to much lower values for both (a) real networks and (b) artificial networks. The initial infection fraction $\rho(0) = 0.4$ and spreading probability $\beta = 0.01$. Symbols and dashed lines represent simulation and theory results, respectively. (c) Size of the jump $J(R_c)$ in $\rho(\infty)$ at the critical resource value R_c. If $J(R_c) = 0$, it means there is a continuous change in the outbreak size with increasing amount of resource devoted. For both real and artificial networks, as the infection rate β increases, the catastrophic jump behavior disappears, switching to a continuous phase.

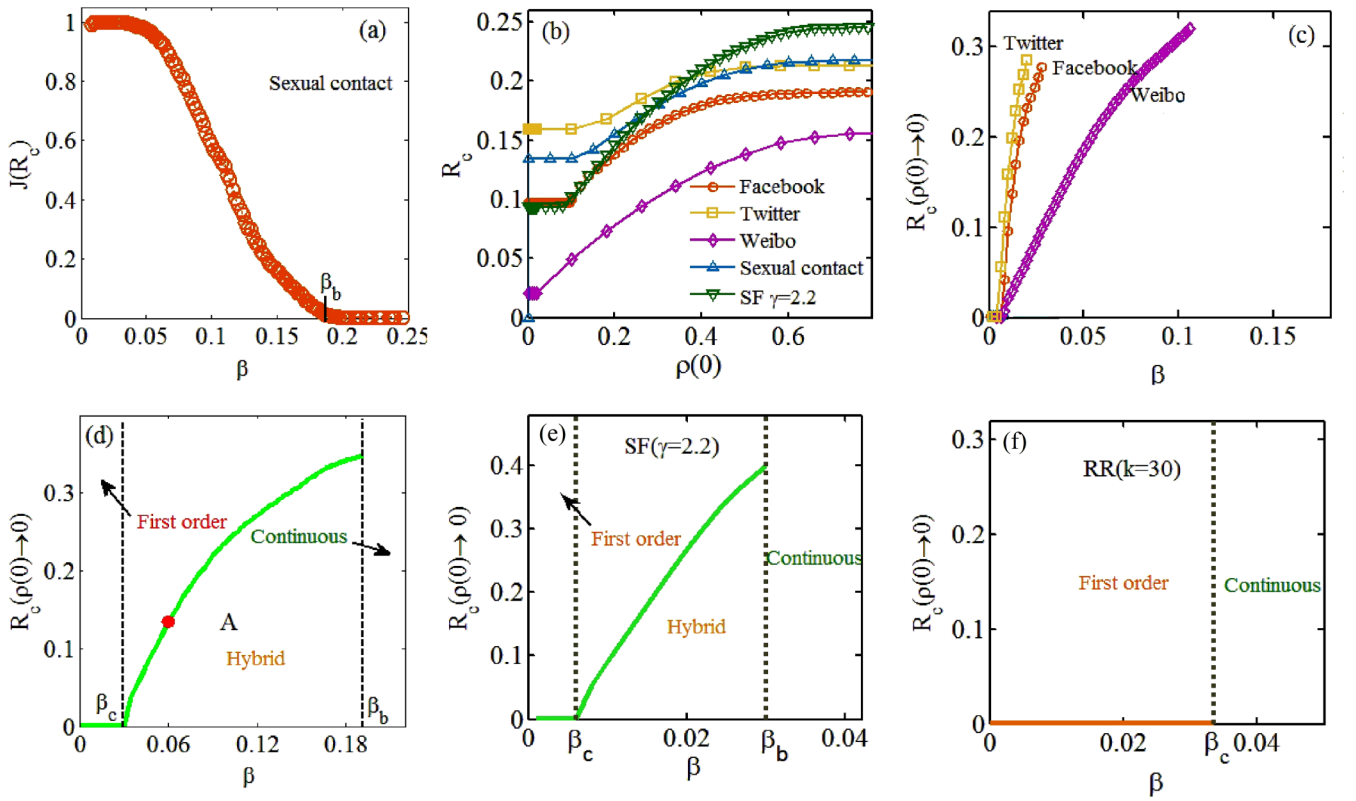

FIG. 6. Nontriviality of the critical resource amount and multiphase behaviors. (a) Size of the jump $J(R_c)$ in $\rho(\infty)$ at the critical resource value R_c as a function of β in the sexual contact network. When the infection rate β is larger than β_b, the catastrophic jump behavior disappears, switching to a continuous phase. (b) For an epidemic disease even with a fraction of initial spreaders close to 0, R_c is significantly larger than 0. This means that even if there is only one initial spreader of the disease, there is a need to set aside at least R_c amount of resource to contain it. Here $\beta = 0.01$ in all simulations. (c–f) Critical resource R_c vs β when $\rho(0) \to 0$ [$\rho(0)$ is very small] for empirical networks and random networks. We divide different phase regions of the sexual contact network (d), the scale-free (SF) network (e), and the random regular (RR) network (f). While the RR network has only two phases—one having a first-order transition and one only continuous change—the sexual contact network and SF network have an additional phase of hybrid transition, in which the infected population abruptly jumps from a nonzero value to a larger value.

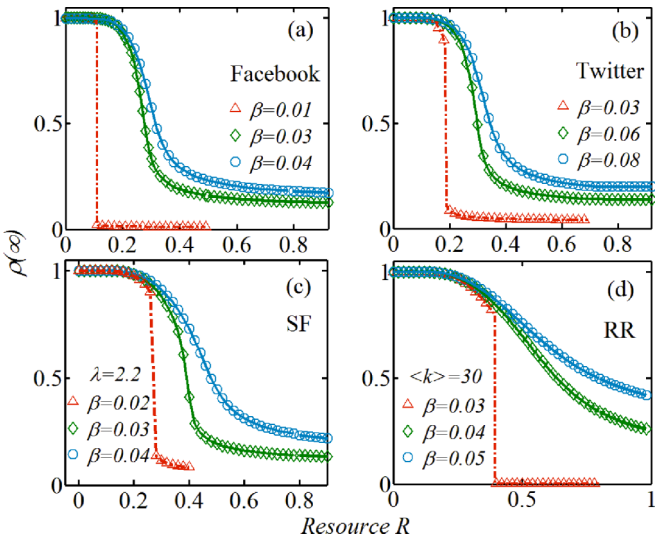

FIG. 7. Discontinuous jump and continuous change of the steady-state infection fraction $\rho(\infty)$ on the social networks (a) Facebook and (b) Twitter and random networks that are (c) scale-free (SF) and (d) random regular (RR). Red, green, and blue symbols represent simulation results at increasing values of β. As β increases, the abrupt jump in $\rho(\infty)$ disappears. When β is small (red), we see a sudden drop in the steady-state infection fraction $\rho(\infty)$ as the resource R increases. There is a difference among the networks. While the Facebook and RR networks show a drop to $\rho(\infty) = 0$, meaning the disease is eradicated, Twitter and the SF network show a drop to $\rho(\infty) > 0$, and $\rho(\infty)$ continues to decrease slowly after that, which corresponds to a hybrid phase transition behavior. As the β value becomes larger (green and blue), the abrupt jump disappears, and the change in $\rho(\infty)$ becomes continuous with increasing R. For all of the networks studied here, the abrupt change disappears with increasing β value. The network sizes are both $N = 20\,000$ in the SF network and random regular network. The minimum and maximum node degrees are $k_{\min} = 10$ and $k_{\max} = 300$ for the SF network.

networks in Fig. 5(c)]. The origin of this first-order phase transition phenomenon can be understood from the theoretical analysis in Sec. II B.

B. Nontriviality of resource amount and multiphase behaviors

Our second main finding concerns heterogenous networks like many real contact networks [5,9,20] having approximately scale-free degree distributions. In these networks, even if there is a single initial infected node [$\rho(0) \to 0$], a significant amount of resource is required to contain the disease. This is shown in Fig. 6(b) as the variation of R_c vs the initial infection fraction $\rho(0)$ for the real social network. For many real networks, the value of R_c at $\rho(0) \to 0$ is significantly larger than 0. This important phenomenon can be understood from Fig. 8(b), as the nonzero solution is obtained from the intersection of the stable (green) and unstable (yellow) solution lines (details in caption).

Our third main result is that we find three types of phase transitions: first order, hybrid, and continuous. The catastrophic transitions such as the first-order and hybrid phase transitions, from spreading dynamics to nonspreading, are induced by the low spreading probability β, which usually corresponds to fatal diseases [30,31]. Figures 6(d) and 6(e) show the three distinct phase transition regimes determined by the value of β for the sexual contact network and the scale-free network. The three phase regimes are separated by β_c and β_b. Here β_c is the critical transmission probability in the original SIS dynamics [10] with the recovery rate equal to 1 (corresponding to $R = +\infty$ in our model). In this scenario, a disease needs to have a β larger than β_c to spread. Therefore when $\beta < \beta_c$, increasing resource R can always eradicate the disease spread. Hence $\beta < \beta_c$ is the region of the first-order phase transition, corresponding to Figs. 8(a) and 8(d). When $\beta > \beta_b$, the infected fraction changes continuously with R, and we call this region the continuous phase, represented in Figs. 8(c) and 8(f). The most interesting region is $\beta_c < \beta < \beta_b$. In this region, since $\beta > \beta_c$, the disease can never be totally removed (even for $R = +\infty$) from the population. At the same time, $\beta < \beta_b$ means that as we increase resource R, the steady state $\rho(\infty)$ will at some point jump from the upper solution to the lower solution [as shown in Figs. 8(b) and 8(e)]. We refer to this region as the *hybrid phase*.

C. Phase transition regimes

Figure 6(e) illustrates the separation of the three distinct phase regimes in the scale-free network and this can also be found in many empirical networks [see Figs. 6(c) and 6(d)]. To investigate the relationship between the presence of these three phases and the degree heterogeneity of the network, we carry out further analysis on scale-free networks with different degree distribution exponents γ, which determine the degree heterogeneity. As shown in Fig. 9(a), for the same value of β, as the degree heterogeneity decreases (with increasing γ), the system evolves from first order to the hybrid phase and, eventually, to a continuous phase. We note that when γ is small, the three phases (continuous, hybrid, and first order) can exist over different values of β, whereas the hybrid phase disappears for large γ. Furthermore, Fig. 9(b) shows that the hybrid phase does not exist in the Erdös-Rényi network.

IV. DISCUSSION

Diseases that are transmitted through water, food, etc., and not directly though individuals, do not directly correspond to the SIS spreading model. However, in their disease spreading process, the effective infectivity will decrease with the increase in the social resource input. This is due to various social effects such as accelerating the discrimination and isolation of the infected, providing clean water and food, decreasing public exposure, improving the public's sanitary habits, and increasing the vaccination rate. In this work, we consider all these effects as the increase in the recovery rate. Obviously, this increased resource's social effect, increased recovery rate, or decreased spreading power is the same and universal for many diseases (including influenza, HIV, etc.) and is not subjected to the spreading dynamics of a specific disease.

In order to further support the conclusions of our model without direct evidence from disease transmission data, we prove that the results reported in our paper are qualitatively the same when the recovery rate increases monotonically with

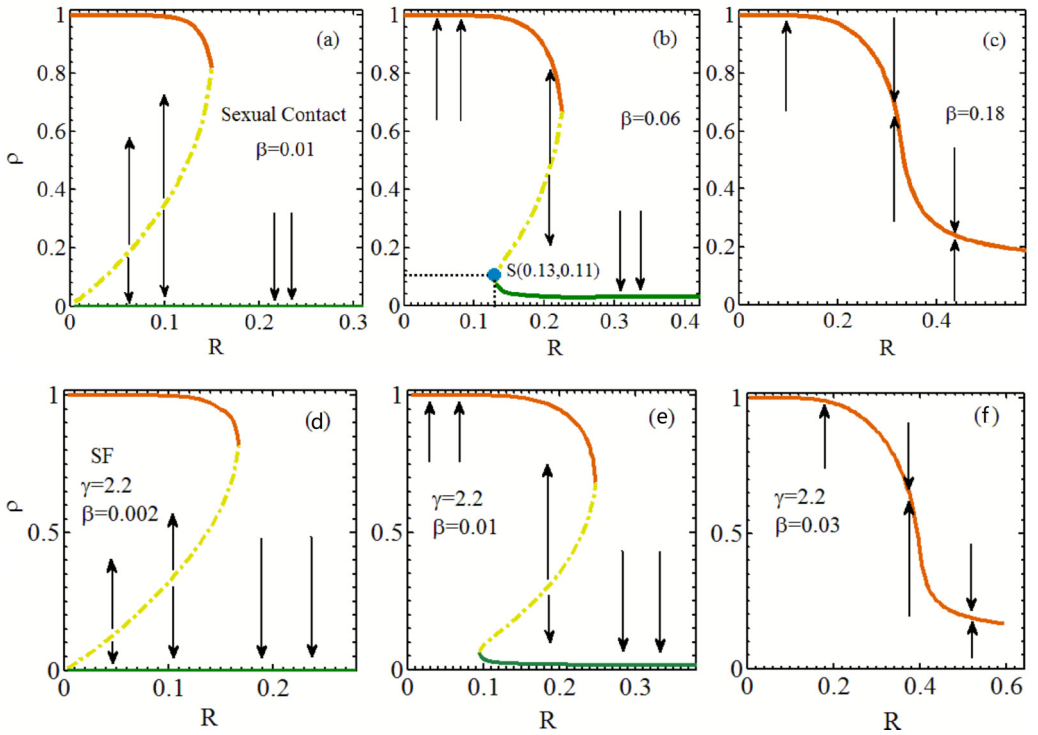

FIG. 8. (a–c) Dynamical stability origin of multiphase behaviors on the sexual contact network. Curves represent the numerical solutions of ρ [i.e., the average of simulated $p_i(\infty)$ values] in the dynamical Eq. (4) for different values of R. For both the first-order transition phase (a) and the hybrid transition phase (b), the upper, orange curve represents the higher steady-state solutions, $\rho_h(\infty)$, and the bottom, green curve represents the lower solutions, $\rho_l(\infty)$. The middle, dashed yellow curve shows the unstable steady-state solution ρ_c. Therefore if the initial fraction of the infected population $\rho(0)$ is above the yellow curve, the system will flow to a higher steady-state value on the orange curve; otherwise, the system will flow to a lower steady-state value on the green curve. Thus, for each ρ value [initial value $\rho(0)$, to be more accurate] in the plot, the yellow curve defines the critical resource R_c. In (b), point S is the lowest point in the dashed yellow line, which means that it leads to a nonzero value of $R_c = 0.13$ when the initial condition is $\rho(0) \in (0, 0.11)$. Such a nonzero R_c when $\rho(0) \to 0$ can be observed in Fig. 6(d), point A (red). This also explains why in Fig. 6(b) the R_c value is flat between $\rho(0) \in (0, 0.11)$. For the continuous phase (c), there is only one stable solution of ρ. Hence there is no abrupt change in the dynamics. (d–f) Corresponding results on the scale-free network. The same three types of dynamical stability phenomenon are found. The network parameters are $N = 20\,000$, $k_{\min} = 10$, $k_{\max} = 300$, and power exponent $\gamma = 2.2$.

the individual resource received. *That is, we have proven that for any recovery rate function whose value is in the range (0,1) and is a monotonic increasing function of* $\frac{R}{\rho}$ *(average shared resource per infectious individual), the main results in the paper remain the same* (see the theoretical analysis in the Appendix).

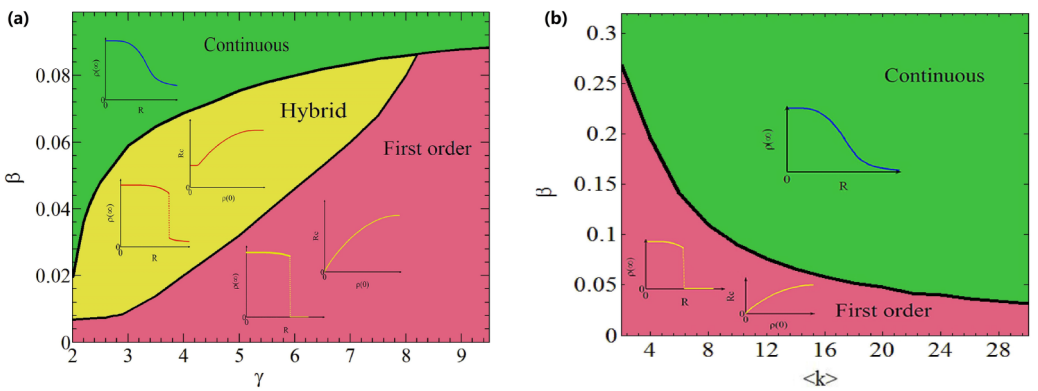

FIG. 9. (a) Phase regimes of the system with different infection rates β and power-law exponents γ in scale-free networks. Both hybrid and first-order phases show an abrupt jump in $\rho(\infty)$ when the amount of resource R decreases. The jump in the first-order phase starts from 0, whereas the one in the hybrid phase starts from a positive value. As the infection rate increases, the system switches to a continuous phase in which no abrupt jump is observed. (b) Phase regimes of the Erdös-Rényi network. The solid line represents the boundary between the first-order transition phase (red) and the continuous phase (green). We see that a larger average degree $\langle k \rangle$ results in a continuous phase, whereas a smaller average degree results in an abrupt change. The network size $N = 20\,000$.

V. CONCLUSION

In this work, we illustrate the impact of resource amount on both artificial and empirical networks, and the results validate the applicability of our theoretical findings. Although the networks used may not be representative of real spreading networks for different diseases, we think that they are representative of both homogeneous and heterogeneous networks. The complicated phase transition behaviors that differ in homogeneous and heterogeneous networks generate rich behaviors in the spreading dynamics. Moreover, our result is not a simple extension of Pastor-Satorras and Vespignani's classic result [10]. First, for all empirical networks, including finite-size scale-free networks (used in the simulation), their propagation thresholds are not 0. Second, for scale-free networks with power-law exponents larger than 3, these networks still require a significant amount of resource to contain epidemics when the initial infectious fraction tends to 0. Third, there is a new threshold on the scale-free network, β_b, which is not in the classic result [10].

There are two important implications for epidemic disease containment. First and foremost, the amount of public resource spent on controlling the spread needs to be higher than a critical value; any amount devoted below this level will be wasted, without a substantial impact on spreading containment. Additionally, any additional amount of resource far above the critical level will bring only a marginal benefit to the containment, as our results indicate that the reduction in the final infected population is indeed small. Second, because many contact networks such as sexual contact networks and social networks are heterogeneous in their degrees, to effectively contain an epidemic disease, even if the initial number of spreaders is very small, we need to set aside a significant amount of resource at the beginning. Any hesitation in devoting enough resource will eventually result in the loss of many lives as well as tremendous public resources. The most fatal diseases measured by the case fatality rate, like Ebola [30] and HIV [31], are among the least infectious in terms of the *basic reproduction number* ($\beta\langle k\rangle$); otherwise they will kill all of their hosts and be unable to reproduce. Therefore, these most fatal diseases tend to show abrupt transitions according to our results, meaning that even a little inadequacy in the devoted public resource can lead to catastrophic outbreaks causing considerable casualties. The effect of the resource on improving the recovery rate can be achieved in a more general sense. For example, during the onset of a disease outbreak, public awareness and disease prevention measures can significantly reduce human contact, which is equivalent to reducing the disease transmission or increasing the curative rate. These social activities, which may also bring the system to an abrupt phase transition, may depend on financial support by the government. Therefore abrupt changes may be more common and relevant in practice. In such cases it is of extreme importance to investigate the resource adequacy in fighting the epidemic disease, preventing it from evolving into a large-scale pandemic.

ACKNOWLEDGMENT

This work was supported by the National Natural Science Foundation of China under Grant No. 61773412, Guangzhou Science and Technology Project, China (Grant No. 201804010473); and Guangdong Research and Development Program in Key Fields, China under Grant No. 2019B020214002.

APPENDIX

1. Data sets

In this section, we list detailed information on the four online social networks and the sexual contact network. In addition, information on the empirical data is listed at the end.

(1) Sexual contact network: The full data set containing the sexual network is downloaded from [20]. It records 50 185 contacts between 6642 escorts and 10 106 sex buyers.

(2) New Orleans Facebook network: The New Orleans Facebook network [32] is downloaded from the Social Computing Group [33]. The network contains 63 392 nodes and 1 633 772 edges.

(3) Twitter network: The social network Twitter [34] is downloaded from the Stanford Large Network Dataset Collection [35]. There are 8106 notes and 2 684 606 edges in the network.

(4) Weibo network: The Weibo data set records the network data of Sina Weibo [36] users in Macau, which was gathered using web crawlers in October 2012 [37]. The network contains 24 023 nodes and 186 753 edges.

(5) Cholera data sets: The data sets of reported cholera cases and deaths (Global Health Observatory data) are downloaded from the website of the World Health Organization [38].

(6) Gross domestic product (PPP) per capita: The gross domestic product (at purchasing power parity) per capita is the PPP value of all final goods and services produced within a country in a given year, divided by the average (or midyear) population for the same year [39]. This data set is downloaded from the World Bank website [40].

(7) Population data: The worldwide population is recorded at the World Bank website [41].

2. Theoretical analysis of a general recovery rate

The analysis in the text considers the case $\mu = e^{-\rho(t)/R}$, but it can be directly generalized to the case where the recovery rate μ takes another explicit form. Now assume that the recover rate $\mu \in [0, 1]$ is a general monotonic increasing function of the variable $\frac{R}{\rho}$. Specifically, we assume $\mu(\rho) = g(\frac{R}{\rho})$, where $g(x)$ is a smooth increasing function defined on $[0, +\infty)$ and satisfies $g(0) = 0, g(+\infty) = 1$. We prove that under these general conditions, the phase behavior is still similar to that in the previous cases. The cases of the random regular network and power-law network are discussed separately.

a. Random regular network

The infected density is governed by the equation $\frac{d\rho}{dt} = f(\rho) = \beta\langle k\rangle\rho(1-\rho) - g(\frac{R}{\rho})\rho$, and $f'(\rho) = \beta\langle k\rangle(1-2\rho) + \frac{R}{\rho}g'(\frac{R}{\rho}) - g(\frac{R}{\rho})$. The equilibrium state, given by $f(\rho) = 0$, is $\rho_0 = 0$ or the solution of the equation $\beta\langle k\rangle(1-\rho) = g(\frac{R}{\rho})$,

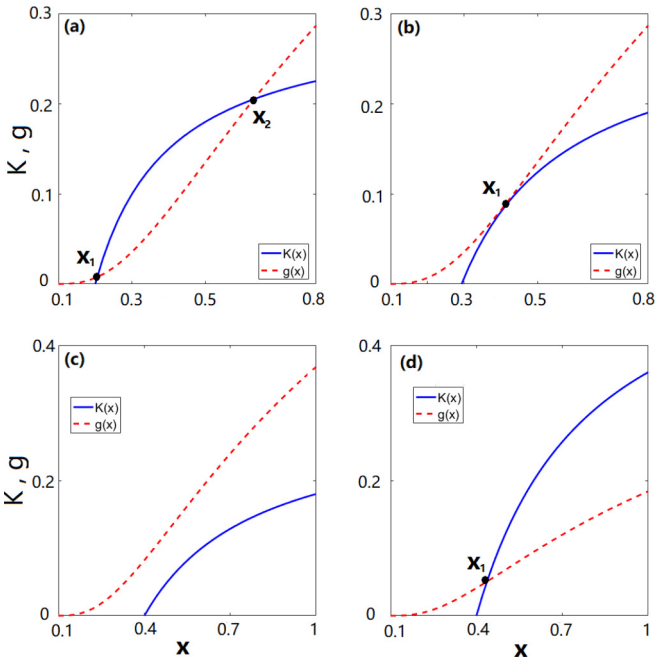

FIG. 10. Relation between curves $K(x)$ and $g(x)$ in the analysis of the random regular network. (a–c) The case of $\beta\langle k\rangle < 1$. (a) For small R, there are two intersection points between $K(x)$ and $g(x)$. (b) Critical value of R where $K(x)$ and $g(x)$ are tangent to each other. (c) For large R, they have no intersection point. (d) The case of $\beta\langle k\rangle > 1$. $K(x)$ and $g(x)$ have one intersection point for all values of R.

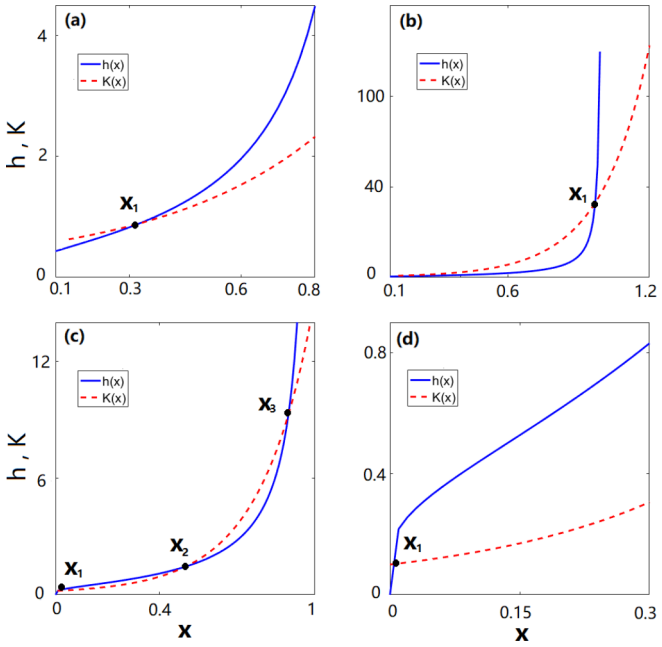

FIG. 11. Relation between curves $K(x)$ and $h(x)$ in the analysis of the power-law network. (a) The case when $\beta\langle k\rangle$ is large. $K(x)$ and $h(x)$ have one intersection point for all values of R. (b–d) The case when $\beta\langle k\rangle$ is small. (b) For large R, $K(x)$ and $h(x)$ have only one intersection point. (d) For small R, they also have only one intersection point. (c) For medium R, they have three intersection points.

$\rho \in (0, 1]$. Now $f'(\rho_0) = \frac{R}{\rho_0} g'(\frac{R}{\rho_0}) - \beta\langle k\rangle\rho_0$, and $f'(\rho_0) < 0$ or $f'(\rho_0) > 0$ implies that it is stable or unstable, respectively.

Define $x = \frac{R}{\rho} \in [R, +\infty)$; then the equation determining the equilibrium state is transformed to $g(x) = \beta\langle k\rangle(1 - \frac{R}{x})$, $x \geqslant R$. Also note that $x_0 = \frac{R}{\rho_0}$; then $f'(\rho_0) < 0 \iff g'(x_0) < \frac{R\beta\langle k\rangle}{x_0^2}$. Now the number of equilibrium states and their stability can be analyzed by a graphic method, i.e., by comparing the figures of $g(x)$ and $K(x) \doteq \beta\langle k\rangle(1 - \frac{R}{x})$ for $x \geqslant R$.

First, consider the case $\beta\langle k\rangle < 1$. Now $f'(0) = \beta\langle k\rangle - 1 < 0$, implying that the zero equilibrium state ρ_0 is stable. Note that $K(+\infty) = \beta\langle k\rangle < 1 = g(+\infty)$ and $K(R) = 0 \leqslant g(R)$. Since $g(x)$ is a smooth general increasing function, from the shape of the function $K(x)$, we know the following fact. When R is small, there are two intersection points, at $x = x_1$ and x_2, with $x_1 < x_2$, referring to Fig. 10(a). Since $g'(x_1) < K'(x_1)$ and $g'(x_2) > K'(x_2)$, the equilibrium $\rho_1 = \frac{R}{x_1}$ is stable while $\rho_2 = \frac{R}{x_2}$ is unstable. When R is large, $g(x)$ and $K(x)$ have no intersection points [Fig. 10(c)], so $\rho_0 = 0$ is the unique equilibrium state in the system. At a critical value $R = R_c$, $g(x)$ and $K(x)$ are tangent to each other, referring to Fig. 10(b). This critical value is the first-order transition point.

Next, consider the case $\beta\langle k\rangle > 1$. Now $K(+\infty) = \beta\langle k\rangle > 1 = g(+\infty)$ and $K(R) = 0 \leqslant g(R)$. For any value of R, there is only one intersection point between $g(x)$ and $K(x)$, at $x = x_1$. And $g'(x_1) < K'(x_1)$ implies that the equilibrium state $\rho_1 = \frac{R}{x_1}$ is stable and $f'(0) = \beta\langle k\rangle - 1 > 0$ implies that the zero equilibrium state $\rho_0 = 0$ is unstable. In this case the phase is continuous.

In summary, we have proven that for random regular networks, when $\beta\langle k\rangle < 1$, there is a first-order transition [Fig. 12(b)], but when $\beta\langle k\rangle > 1$, the phase is continuous [Fig. 12(a)].

b. Power-law network

The graphic analysis method for a power-law network is similar to the case of a random regular network. Let us simply discuss the outline here. With the heterogeneous mean-field approximation approach, we have shown that the final nonzero infected equilibrium state ρ_0 is given by the equation $\Phi(\rho) = \rho$, and $\Phi'(\rho_0) < 1$ or $\Phi'(\rho_0) > 1$ implies that it is stable or unstable. Here, $\Phi(\rho) = \frac{2(e^{\varphi} - \varphi - 1)}{(e^{\varphi} - 1)^2}$ and $\varphi = \frac{2\mu}{\beta\langle k\rangle}$. Since g is a general increasing function, we denote its inverse function $h(x)$, which is a monotonic increasing function defined on $x \in [0, 1)$, with $h(0) = 0$ and $h(1^-) = +\infty$. Now denote $x = g(\frac{R}{\rho}) \in [g(R), +\infty)$; then $\rho = \frac{R}{h(x)}$. Moreover, denote $H(x) = \frac{(e^x - 1)^2}{2(e^x - x - 1)}$, $x \geqslant 0$. It can be easily shown that $H(x)$ is a monotonic increasing function with $H(0) = 1$, $H(+\infty) = +\infty$.

With these notations, the equation $\Phi(\rho) = \rho$ is then transformed to $h(x) = RH(\frac{2x}{\beta\langle k\rangle})$, $x \geqslant g(R)$. Further, denote $K(x) = RH(\frac{2x}{\beta\langle k\rangle})$; then $K(x)$ is obtained from stretching transformation of $H(x)$. Note that $h(g(R)) = R < RH(\frac{2g(R)}{\beta\langle k\rangle}) = K(g(R))$. It can be shown that the parameters R and $\beta\langle k\rangle$ change the shape of the curve of $K(x)$ and the intersection points of $h(x)$ and $K(x)$ and thus affect the phase behavior.

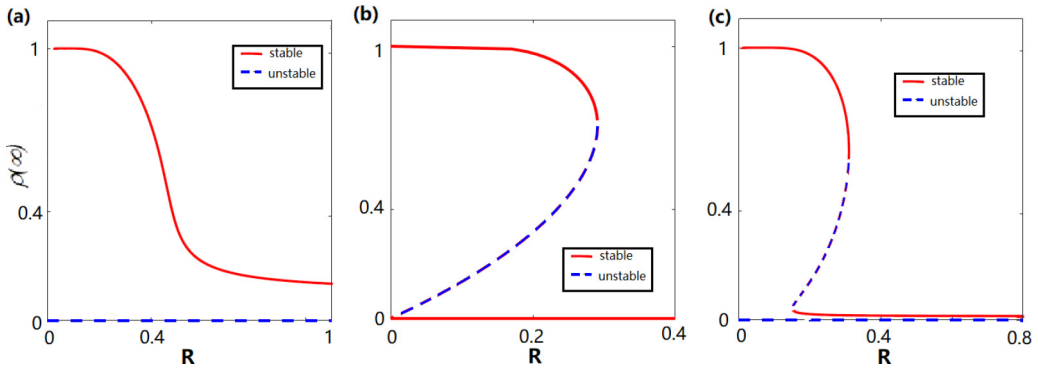

FIG. 12. Diagram of diverse phase behavior. (a) Continuous phase with no phase transition. (b) First-order phase transition. (c) Hybrid phase transition.

The function $K(x)$ is transformed from $H(x)$ by an extension of the x axis and y axis. The larger $\beta\langle k\rangle$ is, the greater the extension of the x axis. Similarly, the larger R is, the greater the extension of the y axis.

For a large $\beta\langle k\rangle$, $K(x)$ is highly extended on the x axis. Thus, for any value of R, $h(x)$ and $K(x)$ have only one intersection point, $x = x_1$, and $k'(x_1) < h'(x_1)$ implies that the corresponding equilibrium point is stable, referring to Fig. 11(a). In this case, the phase is continuous. For a small value of $\beta\langle k\rangle$, $K(x)$ can have more than one intersection point with $h(x)$, depending on the value of R. Most importantly, if R takes a medium value, $h(x)$ and $K(x)$ can have three intersection points, $x_1 < x_2 < x_3$, referring to Fig. 11(c). The equilibrium points corresponding to x_1 and x_3 are stable, while the one corresponding to x_2 is unstable. However, when R is larger than a critical value [Fig. 11(b)] or smaller than a critical value [Fig. 11(d)], $h(x)$ and $K(x)$ have only one intersection point, corresponding to a stable equilibrium. The critical value of R, where $h(x)$ has a tangent point with $K(x)$, is the hybrid (or first-order) phase transition point.

In summary, we have proved that for heterogeneous power-law networks, when $\beta\langle k\rangle$ is small, there is a hybrid (or first-order) transition [Fig. 12(c)], but when $\beta\langle k\rangle$ is large, the phase is continuous [Fig. 12(a)}. The critical values depend on the properties of the network and the recovery rate function.

[1] C. Bell, S. Devarajan, and H. Gersbach, The long-run economic costs of AIDS: Theory and an application to South Africa, Policy Res. Work. Paper **20**, 55 (2003).

[2] D. J. Gubler, Epidemic dengue/dengue hemorrhagic fever as a public health, social and economic problem in the 21st century, Trends Microbiol. **10**, 100 (2002).

[3] J. Sachs and P. Malaney, The economic and social burden of malaria, Nature **415**, 680 (2002).

[4] S. Stewart, N. Murphy, A. Walker, A. McGuire, and J. J. V. McMurray, Cost of an emerging epidemic: An economic analysis of atrial fibrillation in the UK, Heart **90**, 286 (2004).

[5] F. Liljeros, C. R. Edling, L. A. Amaral, H. E. Stanley, and Y. Aberg, The web of human sexual contacts, Nature **411**, 907 (2001).

[6] D. Helbing, Globally networked risks and how to respond, Nature **497**, 51 (2013).

[7] L. Hufnagel, D. Brockmann, and T. Geisel, Forecast and control of epidemics in a globalized world, Proc. Natl. Acad. Sci. USA **101**, 15124 (2004).

[8] V. Colizza, A. Barrat, M. Barthélemy, and A. Vespignani, The role of the airline transportation network in the prediction and predictability of global epidemics, Proc. Natl. Acad. Sci. USA **103**, 2015 (2006).

[9] F. Liljeros, C. R. Edling, and L. A. N. Amaral, Sexual networks: Implications for the transmission of sexually transmitted infections, Microbes Infect. **5**, 189 (2003).

[10] R. Pastor-Satorras and A. Vespignani, Epidemic Spreading in Scale-Free Networks, Phys. Rev. Lett. **86**, 3200 (2001).

[11] R. Parshani, S. Carmi, and S. Havlin, Epidemic Threshold for the Susceptible-Infectious-Susceptible Model on Random Networks, Phys. Rev. Lett. **104**, 258701 (2010).

[12] C. Lagorio, M. Dickison, F. Vazquez, L. A. Braunstein, P. A. Macri, M. V. Migueles, S. Havlin, and H. E. Stanley, Quarantine-generated phase transition in epidemic spreading, Phys. Rev. E **83**, 026102 (2011).

[13] M. Boguná, R. Pastor-Satorras, and A. Vespignani, Absence of Epidemic Threshold in Scale-Free Networks with Degree Correlations, Phys. Rev. Lett. **90**, 028701 (2003).

[14] D. Brockmann and D. Helbing, The hidden geometry of complex, network-driven contagion phenomena, Science **342**, 1337 (2013).

[15] S. V. Scarpino, A. Allard, and L. Hébert-Dufresne, The effect of a prudent adaptive behavior on disease transmission, Nat. Phys. **12**, 1042 (2016).

[16] T. Gross, C. J. D. D'Lima, and B. Blasius, Epidemic Dynamics on an Adaptive Network, Phys. Rev. Lett. **96**, 208701 (2006).

[17] V. Marceau, P. A. Noël, L. Hébert-Dufresne, A. Allard, and L. J. Dubé, Adaptive networks: Coevolution of disease and topology, Phys. Rev. E **82**, 036116 (2010).

[18] D. Wohlfeiler and J. J. Potterat, Using gay men's sexual networks to reduce sexually transmitted disease (STD)/human immunodeficiency virus (HIV) transmission, Sex. Transm. Dis. **32**, S48 (2005).

[19] N. M. Ferguson, D. A. T. Cummings, C. Fraser, J. C. Cajka, P. C. Cooley, and D. S. Burke, Strategies for mitigating an influenza pandemic, Nature **442**, 448 (2006).

[20] L. E. C. Rocha, F. Liljeros, and P. Holme, Simulated epidemics in an empirical spatiotemporal network of 50,185 sexual contacts, PLoS Comput. Biol. **7**, e1001109 (2011).
[21] A. Pandey, K. E. Atkins, J. Medlock, N. Wenzel, J. P. Townsend, J. E. Childs, T. G. Nyenswah, M. L. Ndeffo-Mbah, and A. P. Galvani, Strategies for containing Ebola in West Africa, Science **346**, 991 (2014).
[22] P. E. Lekone and B. F. Finkenstädt, Statistical inference in a stochastic epidemic seir model with control intervention: Ebola as a case study, Biometrics **62**, 1170 (2006).
[23] L. Böttcher, O. Woolley-Meza, N. A. M. Araújo, H. J. Herrmann, and D. Helbing, Disease-induced resource constraints can trigger explosive epidemics, Sci. Rep. **5**, 16571 (2015).
[24] R. J. Webby and R. G. Webster, Are we ready for pandemic influenza? Science **302**, 1519 (2003).
[25] K. Stöhr, The global agenda on influenza surveillance and control, Vaccine **21**, 1744 (2003).
[26] C. Fraser, C. A. Donnelly, S. Cauchemez, W. P. Hanage, M. D. Van Kerkhove, T. D. Hollingsworth, J. Griffin, R. F. Baggaley, H. E. Jenkins, E. J. Lyons *et al.*, Pandemic potential of a strain of influenza A (H1N1): Early findings, Science **324**, 1557 (2009).
[27] D. L. Heymann, *Control of Communicable Diseases Manual* (American Public Health Association, Washington, DC, 2008).
[28] A. C. Davison and D. V. Hinkley, *Bootstrap Methods and Their Application* (Cambridge University Press, Cambridge, UK, 1997), Vol. 1.
[29] T. Poston and I. Stewart, *Catastrophe Theory and Its Applications* (Courier Corporation, Chelmsford, MA, 2014).
[30] G. Chowell and H. Nishiura, Transmission dynamics and control of Ebola virus disease (EVD): A review, BMC Med. **12**, 196 (2014).
[31] G. P. Garnett, The basic reproductive rate of infection and the course of HIV epidemics, AIDS Patient Care Stand. **12**, 435 (1998).
[32] B. Viswanath, A. Mislove, M. Cha, and K. P. Gummadi, On the evolution of user interaction in Facebook, in *Proceedings of the 2nd ACM SIGCOMM Workshop on Social Networks (WOSN'09), Barcelona, Spain* (ACM Press, New York, 2009).
[33] http://socialnetworks.mpi-sws.org/.
[34] J. J. McAuley and J. Leskovec, Learning to discover social circles in ego networks, Adv. Neural Info. Process. Syst. **25**, 548 (2012).
[35] http://snap.stanford.edu/data/egonets-Twitter.html.
[36] http://www.weibo.com.
[37] Y. Hu, S. Ji, Y. Jin, L. Feng, H. E. Stanley, and S. Havlin, Local structure can identify and quantify influential global spreaders in large scale social networks, Proc. Natl. Acad. Sci. USA **115**, 7468 (2018).
[38] http://www.who.int/gho/epidemic_diseases/cholera/en/.
[39] https://en.wikipedia.org/wiki/List_of_countries_by_GDP_(PPP)_per_capita.
[40] http://data.worldbank.org/indicator/NY.GDP.PCAP.PP.CD.
[41] http://data.worldbank.org/indicator/SP.POP.TOTL.